Alpha 1-antitrypsin activates lung cancer cell survival by acting on cap-dependent protein translation, vesicle-mediated transport, and metastasis

Seung-Hee Chang[1,*], Kyung-Cho Cho[2,*], Kyeong-Nam Yu[1], Seong-Ho Hong[1], Sungjin Park[1], Ah Young Lee[1], Sanghwa Kim[1,3], Somin Lee[1,3], Jeong Won Kang[2], Chanhee Chae[4], Jongsun Park[5], Kwang Pyo Kim[2], Myung-Haing Cho[1,3,6,7,8]

[1]Laboratory of Toxicology, College of Veterinary Medicine, Seoul National University, Seoul 151-742, Korea

[2]Department of Applied Chemistry, College of Applied Science, Kyung Hee University, Yongin 463-707, Korea

[3]Graduate Group of Tumor Biology, Seoul National University, Seoul 110-799, Korea

[4]Laboratory of Pathology, College of Veterinary Medicine, Seoul National University, Seoul 151-742, Korea

[5]Department of Pharmacology and Medical Science, Metabolic Diseases and Cell Signaling Laboratory, Research Institute for Medical Sciences, College of Medicine, Chungnam National University, Daejeon 301-747, Korea

[6]Graduate School of Convergence Science and Technology, Seoul National University, Suwon 443-270, Korea

[7]Advanced Institutes of Convergence Technology, Seoul National University, Suwon 443-270, Korea

[8]Institute of GreenBio Science Technology, Seoul National University, Pyeongchang-gun, Gangwon-do 232-916, Korea

[*]These authors have contributed equally to this work

Correspondence to: *Kwang Pyo Kim,* ***email:*** *kimkp@khu.ac.kr*
Myung-Haing Cho, ***email:*** *mchotox@snu.ac.kr*

Keywords: *alpha 1-antitrypsin (AAT), cap-dependent translation, thrombospondin1 (THBS1), cell adhesion molecule (CAM), lung cancer*

Received: *October 26, 2015* ***Accepted:*** *June 12, 2016* ***Published:*** *July 19, 2016*

ABSTRACT

Lung cancer remains the leading cause of cancer-related deaths worldwide. Although elevated expression levels of alpha 1-antitrypsin (AAT) have been reported in lung cancer patients, the precise role of AAT in lung cancer progression and prevention has not yet been fully elucidated. We have explored the mechanisms by which AAT stimulates in lung cancer progression. Here, we used proteomic analyses to compare protein levels following AAT overexpression in normal lung L132 cells containing fundamentally low level of AAT. Overexpression of AAT increased levels of proteins involved in transcription and translation, such as signal transducer and activator of transcription 5B (STAT5B) and eukaryotic translation elongation factor 1-alpha 2 (EEF1A2). Furthermore, dual luciferase activity for cap-dependent protein translation increased a 53% at 24 h and 45% at 48 h in AAT-overexpressing cells compared with control. Overexpression of AAT also increased levels of the vesicular transport protein, GOPC, which inhibited the expression of the autophagy protein, BECN1, thereby possibly increasing cell survival. In addition, overexpression of AAT promoted angiogenesis and cell adhesion through increasing expression of the metastatic protein, thrombospondin 1 (THBS1). In contrast, down-regulation of AAT by short hairpin RNA (shRNA) suppressed cell proliferation, metastasis, and adhesion in human lung adenocarcinoma A549 cells and in the lung tissue of K-*ras*^{LA1} lung cancer model mice. These findings strongly suggest that AAT regulation shows promise as an alternative avenue for lung cancer treatment and prevention.

INTRODUCTION

Alpha 1-antitrypsin (A1AT or AAT), an alpha 1-protease inhibitor (A1PI) and a member of the serine proteinase inhibitor (serpin) superfamily, is a hepatocyte-derived acute phase glycoprotein that inhibits neutrophil elastase [1]. Although elastases do not seem to be evolved for injuring lung tissue, a range of lung diseases, including lung cancer, have been associated with neutrophil elastases. Indeed, the elastin-rich connective tissue framework, a unique characteristic of the lungs, appears to be particularly susceptible to the action of elastolytic proteases [2]. The main function of AAT is to protect lung tissue from enzymes such as neutrophil elastase in inflammatory cells. However, under AAT deficiency or absence, neutrophil elastase breaks down elastin and the lungs lose their elasticity, which results in a diverse range of respiratory diseases.

Recently, elevated plasma and tumor tissue expression levels of AAT have been reported in lung cancer [3, 4]. Moreover, secretomic evidence has demonstrated that AAT is required for cancer cell migration, invasion, and pericellular fibronectin assembly for colonization of lung adenocarcinoma cells [5]. In fact, several lines of evidence show that the C-terminal fragment of AAT induces tumor cell proliferation and invasiveness in human pancreatic adenocarcinoma [6] and breast carcinoma cells [7].

Eukaryotic translation usually initiates protein synthesis through the correlation of certain key proteins bound to the mRNA cap structure. Eukaryotic translation initiation factor 4E (eIF4E) is the cap-binding protein, levels of which have been reported to be substantially elevated in many cancers [8]. In addition, elevated eIF4E greatly facilitates translation of proteins for angiogenesis and growth, such as fibroblast growth factor-2 (FGF-2) and vascular endothelial growth factor (VEGF), and thus promotes tumor formation [9]. The eIF4E-binding protein 1 (4EBP1) is known to inhibit cap-dependent mRNA translation through direct binding with eIF4E translation initiation factor [10]. In fact, our previous study reported that aerosol-delivered 4EBP1 decreased the expression level of eIF4E, leading to inhibition of angiogenesis and endothelial cell proliferation such as FGF-2, VEGF, cluster of differentiation 31 (CD 31, endothelial cell marker or platelet endothelial cell adhesion molecule, PECAM-1), and Ki-67 (cell proliferation marker), thus suppressing lung tumor in a murine lung cancer model [11].

Vesicle-mediated transport is an integral cellular process and the associated proteins play a major role in some important signaling pathways. Golgi-associated PDZ and coiled-coil motif-containing protein (GOPC; also known as PIST, CAL, and FIG) are representative vesicular trafficking proteins that take part in vesicle-mediated transport ER to Golgi, and Golgi to plasma membrane [12]. The PDZ domain of GOPC is known to bind with the carboxy terminus of target proteins such as beclin-1 (BECN1) or glutamate receptor delta-2 (GluD2), and induces autophagy [13, 14]. However, current understanding of the molecular functions of combinatorial vesicle-mediated transport remains limited. Therefore, the potential contribution of this vesicle-mediated transport to malignancy and cancer cell invasiveness should be elucidated.

It has been known that thrombospondin 1 (THBS1) has both pro-metastatic and anti-metastatic properties. THBS1 has been primarily identified to be an endogenous inhibitor of angiogenesis and tumor growth [15]. On the contrary, promotion of cell migration and invasion by THBS1 in human breast carcinoma has also been reported [16]. THBS1 also correlates with a wide range of proteins, such as transforming growth factor-β (TGF-β) [17], matrix metalloproteinase-2 (MMP-2) [18], and matrix metalloproteinase-9 (MMP-9) [19]. An additional study has demonstrated that THBS1 induces cell adhesion molecules (CAM) such as intracellular cell adhesion molecule-1 (ICAM-1) or vascular cell adhesion molecule-1 (VCAM-1) [20].

To summarize, the liver-derived circulating protease inhibitor protein, AAT, has been associated with a protective effect against excessive proteolytic damage in the lung, and its deficiency has been associated with diverse lung diseases. This evidence has prompted us to elucidate the precise role of AAT in lung cancer development, particularly in terms of relevant treatment strategies. Since lung proteins are executors of physiological function and their expression patterns directly reflect various lung diseases, it is therefore important to analyze functions and dynamic patterns of expression that contrast with the fixed nature of the proteins with the aid of proteomics under the influence of AAT. Taking this evidence together, we hypothesized that regulation of AAT may provide clues on how to cope with lung cancer suppression or prevention. Here, we report that AAT activates lung cancer cell survival through promoting cap-dependent translation, vesicular transport, metastasis, and cell adhesion. This strongly suggests that the regulation of the AAT protein may be an alternative treatment for both lung cancer treatment and prevention.

RESULTS

AAT is overexpressed in lung adenocarcinoma tissues and cell lines

In order to determine the expression levels of AAT, RT-PCR, western blot, and confocal laser scanning microscope (CLSM) analyses were carried out in the lungs of human and mouse, and lung cells. AAT levels were significantly increased in human lung tumor samples (adenocarcinoma; especially in stage II) (Figure 1A and 1B) and two adenocarcinoma cells, A549 and NCI-H522

(Figure 1C). The increased level of AAT in A549 cells compared to normal L132 lung cells was further confirmed by CLSM (Figure 1D). Furthermore, AAT level was significantly elevated in the lungs of murine model of human lung adenocarcinoma (K-*ras*^{LA1}) compared to K-*ras* wild-type (WT) mice (Figure 1E). In addition, AAT was also elevated in nicotine-derived nitrosamine ketone (NNK)-induced lung adenocarcinomas of A/J mice (Figure 1F). These observations demonstrated that AAT is overexpressed in lung adenocarcinoma cells and tissues.

Proteomic analysis of differential expressed proteins (DEPs) in AAT-overexpressing L132 cells

Cell lines stably over-expressing the human AAT protein were constructed for studies of the molecular function of AAT in lung cancer progression. The expression level of AAT was evaluated using western blot and immunofluorescence analyses in L132 cells. The results showed an increased AAT protein level in

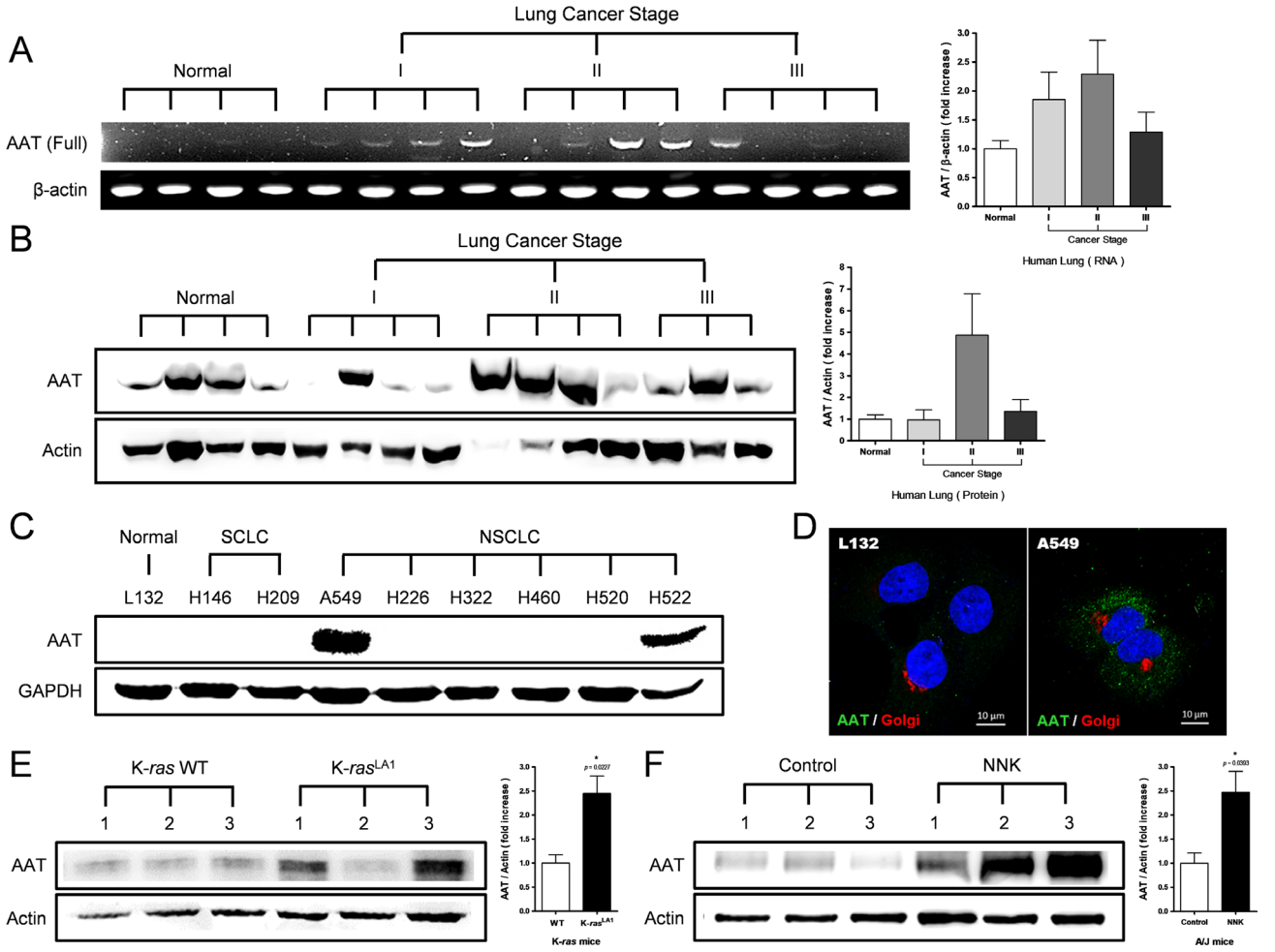

Figure 1: Expression levels of AAT in lung adenocarcinoma tissues and cell lines. A, B. RT-PCR (A) and western blot analyses (B) of AAT in normal human lung tissues and lung adenocarcinoma cancer tissues. Each bar represents the mean ± SEM (n = 4). Normal = normal lung tissues; I = lung cancer stage I adenocarcinoma tissues; II = lung cancer stage II adenocarcinoma tissues; and III = lung cancer stage III adenocarcinoma tissues. **C.** AAT protein expression in several lung cell lines determined by western blot analysis. Cell lysates were subjected to western blot analysis. Blot was probed with antibody of AAT. L132 = normal lung cells; H146 and H209 = small cell lung cancer (SCLC) cells; A549, H226, H322, H460, H520, and H522 = non-small cell lung cancer (NSCLC) cells. **D.** Fluorescence imaging of AAT in L132 and A549 cells. Cells were incubated for 48 hours, followed by fixing and immunostaining for AAT (green *via* Alexa Fluor 488), Golgi apparatus (red *via* CellLight Reagents BacMam 2.0), and nuclei (blue *via* DAPI). The scale bars represent 10 μm. **E, F.** AAT protein expressions and densitometric analyses in the lungs of K-*ras*^{LA1} (14 weeks) (E) and NNK-treated mice (19 weeks) (F). K-ras WT = K-ras wild type; K-*ras*^{LA1} = Human lung adenocarcinoma model mice; Control = A/J mice injected with saline; NNK = A/J mice injected with NNK. Values are the means ± SEM (n = 3). $^{*}p<0.05$ *vs.* WT (K-*ras* mice) or Control (A/J mice).

stably AAT up-regulated cells (AAT) compared to that in the vector-transfected (Vec) and control cells (Con) (Supplementary Figure S1A and S1B). To gain greater insight into the changes associated with overexpression of AAT in L132 cells compared to reference cells, the Tandem Mass Tag (TMT) labeling quantitative proteomic analyses were performed, and a total of 8,709 proteins were identified and quantified through the triplicate MS analysis (Supplementary Figure S1C). The protein ratios, and ratio *p* value and sample *p* value for each quantitated protein estimating technical variability were calculated using the R software package Isobar (Isobar released Sep_2014, http://bioinformatics.cemm.oeaw.ac.at). Proteins were selected as differentially expressed proteins (DEPs) when both the ratio *p* value and sample *p* value were under 0.05 in AAT/Con or AAT/Vec in at least one replicate (Figure 2A and Supplementary Figure S2). In order to investigate the biological process changes associated with AAT overexpression, gene ontology (GO) analysis of biological processes from DEPs were performed using DAVID Bioinformatics resources [21]. The significantly enriched GO annotations when they had *p* values under 0.05 in Fisher's exact test were selected, and among the enriched biological process, significant terms are shown in Table 1. Interestingly, the most obvious enriched GO terms of up-regulated DEPs were vesicle-mediated transport, regulation of cell death, and regulation of cell adhesion. In contrast, mitochondrial function-related GO terms such as energy derivation by oxidation of organic compounds were enriched in down-regulated DEPs.

Elevated AAT facilitates cell survival through the increase of cap-dependent protein translation, vesicle-mediated transport, and negative regulation of cell death

In order to confirm the potential effect of AAT on transcription and protein translation, the expression levels of signal transducer and activator of transcription 5B (STAT5B) and eukaryotic translation elongation factor 1α2 (EEF1A2) in AAT-overexpressing cells were evaluated. Increased STAT5B and EEF1A2 protein levels were shown by western blot and densitometric analysis (Figure 2B). In order to determine AAT-mediated regulation of cap-dependent protein translation, western blot and dual-luciferase assays were carried out in AAT-overexpressing cells. Western blot revealed an increased phosphorylation of eIF4E and 4EBP1 compared to control and vector-transfected cells (Figure 2C). Dual luciferase assay demonstrated that phosphorylation of eIF4E and 4EBP1 strongly was well correlated with the pattern of cap-dependent protein translation; in AAT-overexpressing cells, cap-dependent translation was increased by 53% and 45% compared to control cells at 24 and 48 hours, respectively (Figure 2D). In order to determine the effect of increased AAT on proliferation, xCELLigence (Roche) was used to measure real-time cell proliferation. A significant increase in proliferation was observed in AAT-overexpressing cells compared to control and vector-transfected cells (Figure 2E). The densitometric bar graph was well correlated with that of the xCELLigence results at 48 hours (Figure 2E, *right panel*).

To confirm the proteomics result of vesicle-mediated transport, expression levels of GOPC and the related autophagy protein, BECN1, were re-confirmed by western blot. An increased GOPC expression level at 24 and 48 hours was shown in AAT-overexpressing cells, whereas a decrease of BECN1 level was observed (Figure 2F). Induction of GOPC at 24 hours was further confirmed by immunofluorescence assay (Supplementary Figure S3A). To further confirm AAT-mediated regulation of GOPC expression, AAT C-terminus (functional site of the AAT) deletion mutant (AAT-mt) was used. The expression level of GOPC was increased in AAT-overexpressing cells, whereas no increase was observed in AAT-mt cells (Supplementary Figure S3B). Immunoprecipitation (IP) assay revealed clear evidence of binding between GOPC, Golgi-associated protein, and BECN1 (Supplementary Figure S3C). Moreover, *in situ* proximity ligation assay (PLA) also confirmed the binding affinity of these two proteins in stable AAT up-regulated L132 cells as shown in Supplementary Figure S3D. GM130, a *cis*-Golgi marker, was used as a marker of Golgi apparatus. Furthermore, the effect of AAT on vesicle-mediated transport was evaluated in AAT-overexpressing cells. As shown in Figure 2G, induction of mannose-6-phosphate receptor (M6PR; transport phosphorylated lysosomal enzymes from Golgi complex and the cell surface to pre-lysosomal compartments) and clathrin (plays a major role in the formation of coated vesicles) was observed by immunofluorescence assay. The red fluorescence intensity of each protein was measured using the Image J software.

Human Bcl-2 is an anti-apoptotic, membrane-associated oncoprotein that can promote cell survival by blocking the release of the cytochrome *c* through stabilization of the mitochondrial membrane [22]. Bcl-2 also inhibits BECN1-dependent autophagy, and thus helps cell survival [23]. Our results showed that the increase of Bcl-2 and decrease of cytochrome *c* and LC3B in AAT-overexpressing cells (AAT) compared to vector (Vec) and control (Con) cells (Figure 2H). To confirm the decrease of autophagy by AAT, chloroquine (CQ), used to measure autophagic flux in stable AAT up-regulated L132 cells. The about 41 % increase on LC3II expression in control cell, whereas, 25 % increase in AAT-overexpressing cell obtained by autophagy inhibition. BECN1 did not detected this pattern. Furthermore, the decreases of cytochrome *c* release from mitochondrial membrane into the cytosol (Figure 2J), Complex IV (COX IV; or cytochrome *c* oxidase), and caspase-3 activity were observed in AAT-overexpressing L132 cells (Figure 2K and 2L). Moreover,

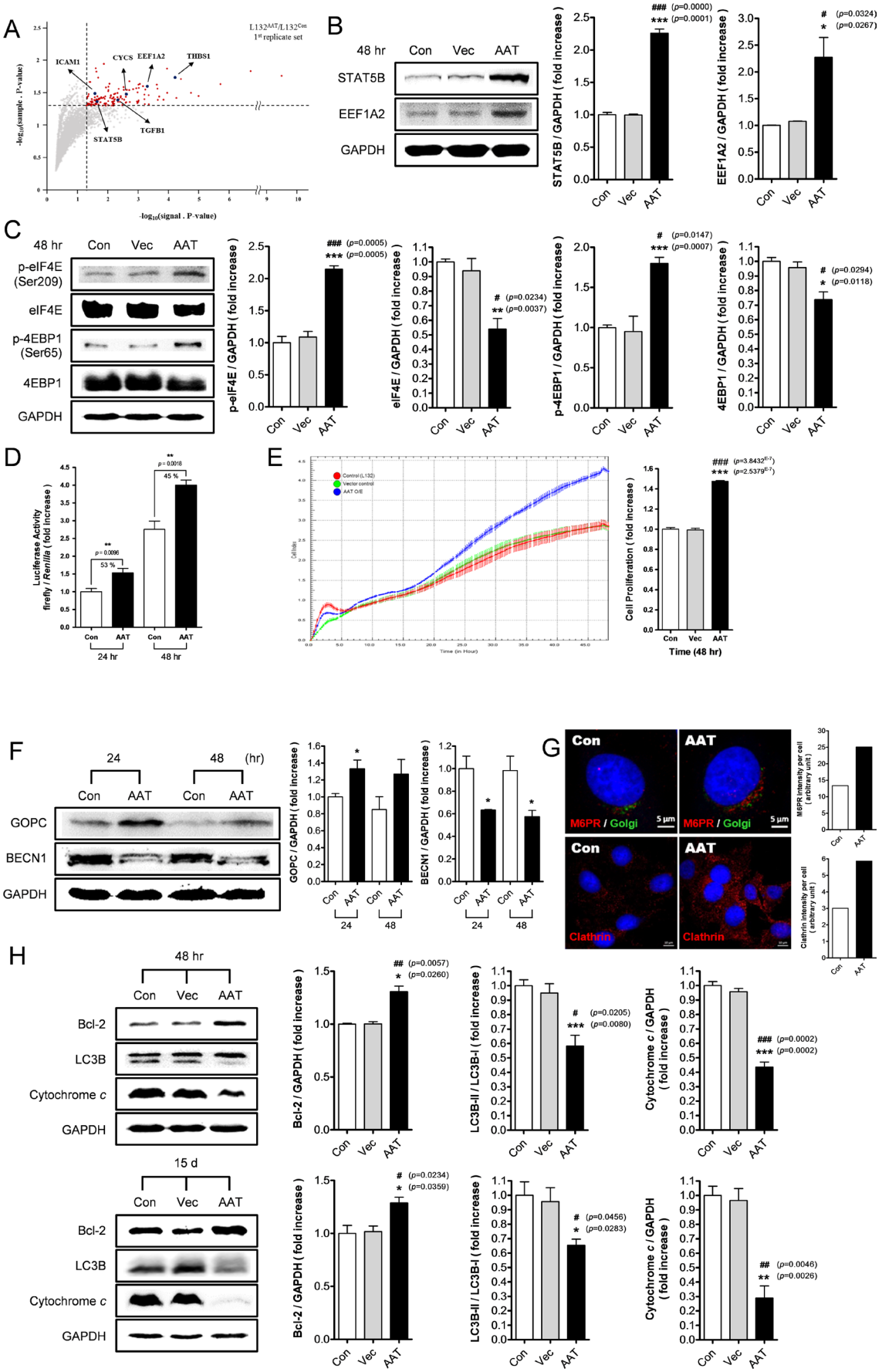
A
B
C
D
E
F
G
H
48 hr
Con
Vec
AAT
STAT5B
EEF1A2
GAPDH
p-eIF4E (Ser209)
eIF4E
p-4EBP1 (Ser65)
4EBP1
24 hr
48 hr
15 d
Bcl-2
LC3B
Cytochrome c
M6PR / Golgi
Clathrin
Cell Proliferation (fold increase)
Time (48 hr)

(*Continued*)

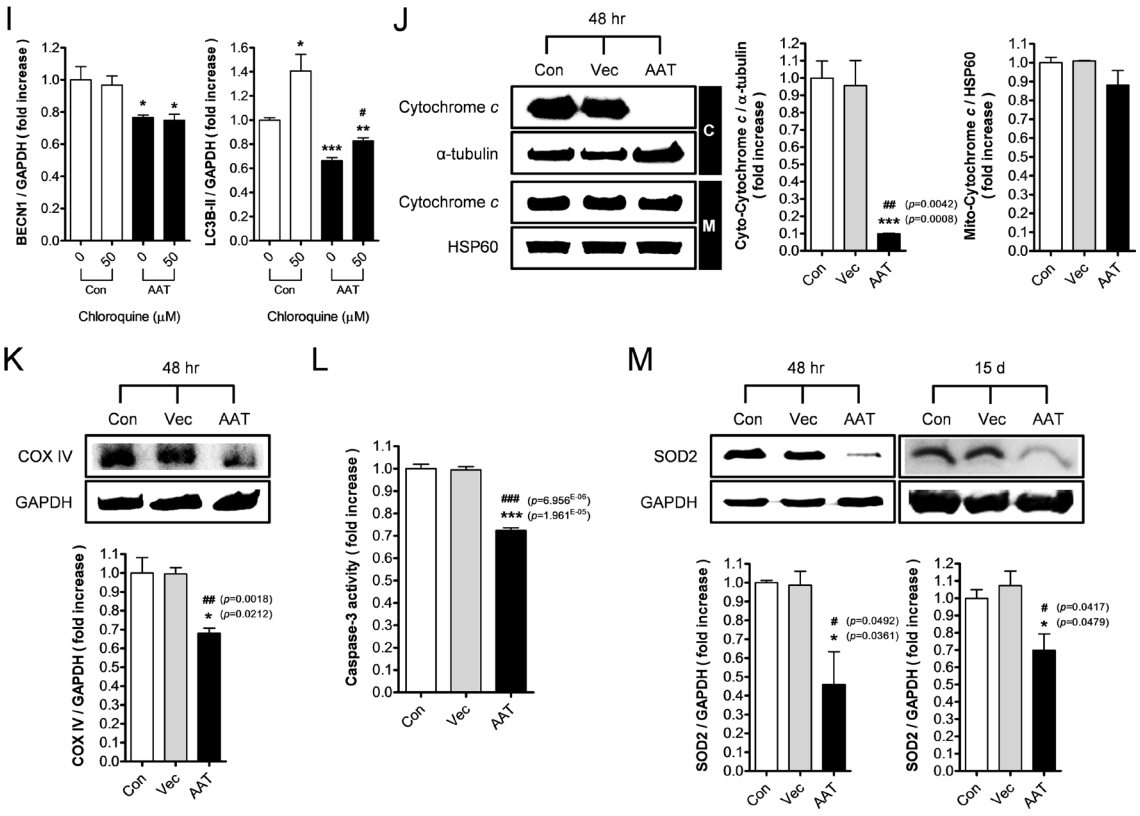

Figure 2: Effects of AAT on protein translation, cell proliferation, vesicle-mediated transport, and cell survival in normal human lung cell L132. A. Volcano plot representation of significantly up- or down-regulated proteins in AAT/Con 1st replicate set. Dashed lines delimit differential expressed proteins (*red* and *blue* dot). **B.** Western blot analyses of STAT5B and EEF1A2. Cell lysates were subjected to western blot analysis. Blots were probed with antibody of STAT5B or EEF1A2. Con = L132 cell; Vec = vector control; AAT = AAT overexpression. *Right panel*) Densitometric analyses of the STAT5B and EEF1A2 western blot result. Values are the means ± SEM (n = 3). $^{*}p$<0.05 or $^{***}p$<0.001 *vs.* Con; $^{\#}p$<0.05 or $^{\#\#\#}p$<0.001 *vs.* Vec. **C.** Effect of AAT on protein translation. Cell lysates were subjected to western blot analysis. Blots were probed with antibodies as indicated. *Right panel*) Densitometric analyses of translation-related proteins. Values are the means ± SEM (n = 3). $^{*}p$<0.05, $^{**}p$<0.01 or $^{***}p$<0.001 *vs.* Con; $^{\#}p$<0.05 or $^{\#\#\#}p$<0.001 *vs.* Vec. **D.** Effect of AAT on cap-dependent translation. Cells were transfected with bicistronic reporter construct, pcDNA-fLuc-polIRES-rLuc, and incubated for 24 or 48 hours. Values are the means ± SEM (n = 5). $^{**}p$<0.01 *vs.* Con. **E.** Real-time cell proliferation assay in L132 cells with overexpressed AAT, vector control, or control. Stably expressed cells were measured using an xCELLigence system for 48 hours. *Right panel*) Cell proliferation result at 48 hours in L132 cells with overexpressed AAT, vector control, or control. Values are the means ± SEM (n = 4). $^{***}p$<0.001 *vs.* Con (*red line*), $^{\#\#\#}p$<0.001 *vs.* Vec (*green line*). **F.** Effects of AAT on GOPC and BECN1 expression. Cell lysates were subjected to western blot analysis. Blots were probed with antibodies as indicated. *Right panel*) Densitometric analyses of the GOPC and BECN1 western blot result. Values are the means ± SEM (n = 3). $^{*}p$<0.05 *vs.* Con of each time. **G.** Effect of AAT on vesicle-mediated transport. Stably expressed cells were incubated for 24 hours, followed by fixing and immunofluorescence for M6PR or Clathrin (red *via* Alexa Fluor 555) and nuclei (blue *via* DAPI). Immunostaining of GM130 (green *via* Alexa Fluor 488) displays Golgi apparatus, and the scale bars represent 10 μm. *Right panel*) Quantitative result of M6PR or Clathrin expression. Data represent the intensity of M6PR or Clathrin/cell. **H.** Effect of AAT on apoptosis- or autophagy-related protein. Cell lysates were subjected to western blot analysis. Blots were probed with indicated antibodies. *Right panel*) Densitometric analyses of the Bcl-2, LC3B, and cytochrome *c* western blot result. Values are the means ± SEM (n = 3). $^{*}p$<0.05, $^{**}p$<0.01 or $^{***}p$<0.001 *vs.* Con; $^{\#}p$<0.05, $^{\#\#}p$<0.01 or $^{\#\#\#}p$<0.001 *vs.* Vec. **I.** Effect of chloroquine on AAT-induced BECN1 and LC3B expression. Cells were treated with chloroquine (50 μM) for 1 hour. Cell lysates were subjected to western blot analysis of BECN1 and LC3B, and densitometric analyses of the western blot results were performed. Values are the means ± SEM (n = 3). $^{*}p$<0.05, $^{**}p$<0.01 or $^{***}p$<0.001 *vs.* Con (CQ, 0 μM); $^{\#}p$<0.05 *vs.* AAT (CQ, 0 μM). **J.** Effect of AAT on cytochrome *c* release. Mitochondria and cytosolic cell fractions were subjected to western blot analysis. Blots were probed with cytochrome *c* antibody. HSP60 and α-tubulin were used as a loading control for mitochondria and cytosol, respectively. *Right panel*) Densitometric analyses of the cytochrome *c* western blot result. Values are the means ± SEM (n = 3). $^{***}p$<0.001 *vs.* Con, $^{\#\#}p$<0.01 *vs.* Vec. **K.** Effect of AAT on COX IV protein expression. Cell lysates were subjected to western blot analysis. Blots were probed with antibody of COX IV. *Lower panel*) Densitometric analysis of the COX IV western blot result. Values are the means ± SEM (n = 3). $^{*}p$<0.05 *vs.* Con, $^{\#\#}p$<0.01 *vs.* Vec. **L.** Effect of AAT on caspase-3 activity. Cell lysates were subjected to Caspase 3 Assay Kit and direct caspase-3 activity was measured using an Epoch microplate spectrophotometer. Values are the means ± SEM (n = 4). $^{***}p$<0.001 *vs.* Con, $^{\#\#\#}p$<0.001 *vs.* Vec. **M.** Effect of AAT on SOD2 protein expression. Cell lysates were subjected to western blot analysis. Blots were probed with antibody of SOD2. *Lower panel*) Densitometric analysis of the SOD2 western blot result. Values are the means ± SEM (n = 3). $^{*}p$<0.05 *vs.* Con, $^{\#}p$<0.05 *vs.* Vec.

Table 1: Summary of protein list within GO annotation

	Expression log2 (AAT/Con) replicate #1, #2, #3	Expression log2 (AAT/Vec) replicate #1, #2, #3
"Regulation of Cell Death"		
Elongation factor 1-alpha 2 (EEF1A2)	***1.04***, ***1.04***, ***1.17***	***0.98***, 1.14, 1.32
Signal transducer and activator of transcription 5B (STAT5B)	***0.61***, 0.37, 0.43	***0.58***, 0.45, 0.52
Thrombospondin-1 (THBS1)	***0.68***, N/D, N/D	***1.33***, N/D, N/D
"Vesicle-mediated Transport"		
Golgi-associated PDZ and coiled-coil motif-containing protein (GOPC)	***0.35***, ***0.33***, 0.14	0.26, 0.24, 0.14
Transforming growth factor-beta 1 (TGF-β1)	***0.46***, 0.15, 0.17	***0.62***, 0.28, ***0.53***
"Regulation of Cell Adhesion"		
Intercellular adhesion molecule-1 (ICAM-1)	-0.03, -0.17, -0.41	***0.77***, ***0.48***, ***1.25***
"Energy Derivation by Oxidation of Organic Compounds"		
Cytochrome *c* (CYCS)	***-0.50***, -0.43, ***-0.47***	***-0.68***, ***-0.54***, ***-0.57***
Superoxide dismutase [Mn], mitochondrial (SOD2)	***-0.55***, -0.42, -0.47	***-0.63***, ***-0.52***, ***-0.69***

This list includes ratio information in AAT overexpressed. *bold italic ratio means the sample *p* value and signal *p* value < 0.05 in replicate.

up-regulation of AAT increased cell survival even 15 days of starvation (Supplementary Figure S4A). The distinct pink color medium of AAT-overexpressing cells, seen in Supplementary Figure S4B, is an indirect signal of cell survival under poor nutrition (the media were not changed for 15 days of test period). This demonstrated that AAT-overexpressing cells could survive longer compared to control cells, for which the color of media appeared a paler pink color. In additionally, the expression level of manganese superoxide dismutase (MnSOD; SOD2), which is known to be a tumor suppressive protein via inhibition of cell proliferation and induction of apoptosis [24], was also reduced in AAT-overexpressing L132 cells (Figure 2M). Together, our observations demonstrated that up-regulation of AAT facilitated cell survival through the promotion of cap-dependent protein translation, vesicle-mediated transport, and negative regulation of cell death.

AAT promotes angiogenesis and cell adhesion through regulating of thrombospondin 1

Furthermore, the effect of AAT on angiogenesis was evaluated using human angiogenesis array and densitometric analysis in stably AAT over-expressed L132 cells. The expression levels of representative angiogenesis-related proteins were significantly increased in AAT-overexpressing L132 cells (AAT) compared to control cells (Con) (Figure 3A). Again, increased THBS1 level was confirmed at 15 days (Figure 3B). Moreover, the induction of THBS1 was closely associated with AAT because AAT-mt did not increase THBS1 protein expression (Figure 3C). In addition, the increase of ICAM-1 in AAT-overexpressing cells re-confirmed the proteomics result (Figure 3D), and increased levels of ICAM-1 and FGF-2 by AAT-overexpression were also confirmed using AAT-mt (Figure 3E). To confirm THBS1-mediated regulation of ICAM-1 or FGF-2 expression on AAT-overexpressing condition, THBS1 inhibitor, LSKL, was employed. The over-expression of THBS1, ICAM-1 and FGF-2 were inhibited with LSKL treatment (Figure 3F). Cell adhesion assay was supported the western blot results of cell adhesion protein (Figure 3G). Together, our observations demonstrated that up-regulation of AAT induced angiogenesis and cell adhesion through regulation of THBS1.

Down-regulation of AAT suppresses cell proliferation through regulation of cap-dependent protein translation and cell death in human lung cancer cells

To determine the effect of decreased AAT on cancer cell proliferation and cap-dependent protein translation, RT-PCR, western blot, real-time cell

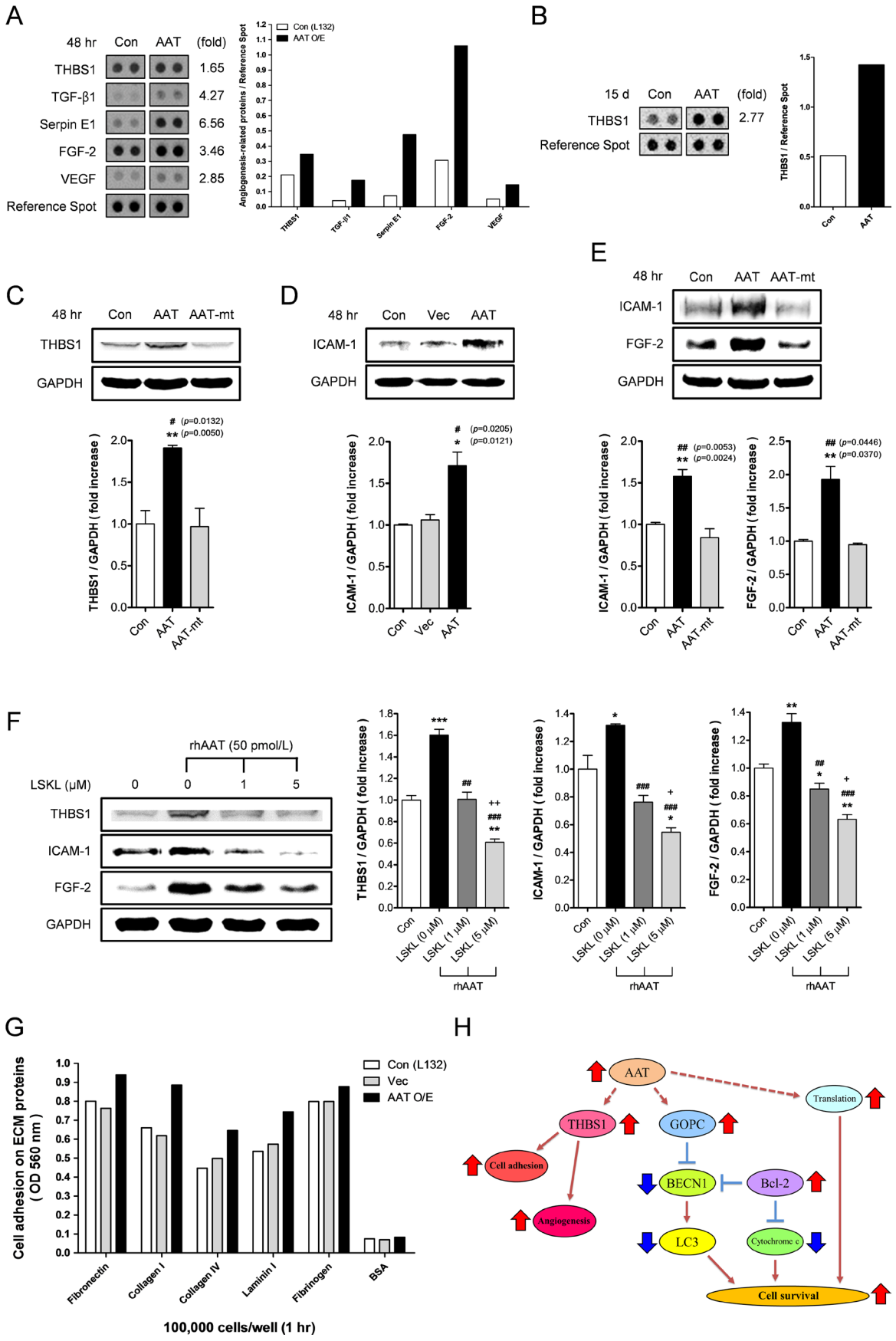
A
48 hr
Con
AAT
(fold)
THBS1
1.65
TGF-β1
4.27
Serpin E1
6.56
FGF-2
3.46
VEGF
2.85
Reference Spot
Con (L132)
AAT O/E
Angiogenesis-related proteins / Reference Spot
B
15 d
Con
AAT
(fold)
THBS1
2.77
Reference Spot
THBS1 / Reference Spot
C
48 hr
Con
AAT
AAT-mt
THBS1
GAPDH
THBS1 / GAPDH (fold increase)
D
48 hr
Con
Vec
AAT
ICAM-1
GAPDH
ICAM-1 / GAPDH (fold increase)
E
48 hr
Con
AAT
AAT-mt
ICAM-1
FGF-2
GAPDH
ICAM-1 / GAPDH (fold increase)
FGF-2 / GAPDH (fold increase)
F
rhAAT (50 pmol/L)
LSKL (μM)
0
0
1
5
THBS1
ICAM-1
FGF-2
GAPDH
THBS1 / GAPDH (fold increase)
ICAM-1 / GAPDH (fold increase)
FGF-2 / GAPDH (fold increase)
Con
LSKL (0 μM)
LSKL (1 μM)
LSKL (5 μM)
rhAAT
G
Cell adhesion on ECM proteins (OD 560 nm)
Con (L132)
Vec
AAT O/E
Fibronectin
Collagen I
Collagen IV
Laminin I
Fibrinogen
BSA
100,000 cells/well (1 hr)
H
AAT
Translation
THBS1
GOPC
Cell adhesion
BECN1
Bcl-2
Angiogenesis
LC3
Cytochrome c
Cell survival

(*Continued*)

Figure 3: Effects of AAT on angiogenesis and cell adhesion in normal human lung cell L132. A. Effect of AAT on angiogenesis-related proteins. Cell lysates were subjected to human angiogenesis array and the bands-of-interest were visualized using Ez-Capture MG. *Right panel*) Quantitative result of the angiogenesis array. Data represent the density of the indicated proteins/reference spot. Con = L132 cell; AAT = AAT overexpression. **B.** Effect of AAT on THBS1 protein expression. Cell lysates were subjected to human angiogenesis array. *Right panel*) Quantitative result of THBS1 expression. Data represent the density of THBS1 proteins/reference spot. **C.** Conformation of THBS1 induction by AAT. AAT-C44 deletion mutant (AAT-mt) expressed stable cell was used for western blot of THBS1. *Lower panel*) Densitometric analysis of the THBS1 western blot result. Values are the means ± SEM (n = 3). $^{**}p$<0.01 *vs.* Con, $^{\#}p$<0.05 *vs.* AAT-mt. **D.** Effect of AAT on ICAM-1 protein expression. Cell lysates were subjected to western blot analysis. Blots were probed with antibody of ICAM-1. *Lower panel*) Densitometric analysis of the ICAM-1 western blot result. Values are the means ± SEM (n = 3). $^{*}p$<0.05 *vs.* Con, $^{\#}p$<0.05 *vs.* Vec. **E.** Conformation of ICAM-1 and FGF-2 induction by AAT. AAT-C44 deletion mutant (AAT-mt) expressed stable cell was used for western blot of ICAM-1 and FGF-2. *Lower panel*) Densitometric analysis of the ICAM-1 and FGF-2 western blot result. Values are the means ± SEM (n = 3). $^{**}p$<0.01 *vs.* Con, $^{\#\#}p$<0.01 *vs.* AAT-mt. **F.** Effect of THBS1 inhibitor, LSKL, on ICAM-1 and FGF-2 protein expression in AAT-induced condition. Cells were co-treated with the recombinant human AAT (rhAAT; 50 pmol/L) and LSKL (1 or 5 μM) for 48 hours. Cell lysates were subjected to western blot analysis. Blots were probed with antibodies as indicated. *Right panel*) Densitometric analyses of the THBS1, ICAM-1, and FGF-2 western blot result. Values are the means ± SEM (n = 3). $^{*}p$<0.05, $^{**}p$<0.01 or $^{***}p$<0.001 *vs.* Con; $^{\#\#}p$<0.01 or $^{\#\#\#}p$<0.001 *vs.* LSKL (0 μM); ^{+}p<0.05 or ^{++}p<0.01 *vs.* LSKL (1 μM). **G.** Effect of AAT on cell adhesion. Cell lysates were subjected to CytoSelect™ 48-Well Cell Adhesion Assay Kit and stained/adhesion cell was measured using an Epoch microplate spectrophotometer. **H.** Schematic signal pathway by which AAT affects in L132 cells. Based on our studies, AAT takes part in lung cancer cell survival through promoting cap-dependent translation, vesicular transport, angiogenesis, and cell adhesion.

proliferation using xCELLigence, and dual-luciferase assays were carried out in A549 cells with stable AAT down-regulation. At first, decreased mRNA and protein levels of AAT by shRNA construct against human AAT were confirmed by RT-PCR, western blot, and densitometric analyses in AAT down-regulating cell (shAAT) compared to scramble-transfected (shScr) and control (Con) cells (Figure 4A and 4B). Transcription and translation proteins-STAT5B and EEF1A2 levels that were up-regulated by AAT overexpression were decreased in shAAT-transfected cells (Figure 4C, compare to Figure 2B). Decreased cancer cell proliferation and cap-dependent protein translation were also observed in AAT down-regulating cells (Figure 4D-4F). In order to determine whether down-regulation of AAT was associated with autophagy and apoptosis, western blot analyses of Bcl-2, cytochrome *c*, and LC3B were performed in shAAT-transfected cells. Down-regulated AAT function caused an increase of cytochrome *c* and LC3B and a decrease of Bcl-2 (Figure 4G). Moreover, the effect of down-regulated AAT on cell morphology was observed using Eclipse Ti-S inverted microscope (Nikon, Tokyo, Japan). As shown in Supplementary Figure S5, control A549 cells were growing well (*blue circles*) for 15 days whereas AAT down-regulating cells were not (*red dot lines* represent interface between each colony). Furthermore, although the reduction of SOD2 was observed in AAT-overexpressing L132 cells, AAT down-regulation caused the reverse phenomena as excessive overexpression in stably shAAT-transfected A549 cells (Figure 4H, compare to Figure 2I). These observations demonstrated that down-regulation of AAT suppressed cell survival through controlling the cap-dependent protein translation, autophagy, and apoptosis.

Down-regulation of AAT suppresses angiogenesis, migration, invasion, and cell adhesion in human lung cancer cells

To determine the effect of decreased AAT on angiogenesis, human angiogenesis array and western blot analysis were used to assess stable AAT down-regulating cells. The expression levels of angiogenesis-related proteins were decreased 4 ~ 58% at 96 hours in AAT down-regulating A549 cells (shAAT) compared with control (Con) cells (data not shown). Furthermore, western blot and densitometric analysis revealed that the expression levels of THBS1 and FGF-2 were decreased at 7 days (Figure 5A). The expression level of AAT was increased in the lungs of NNK-treated mice (Figure 1F). Therefore, in order to elucidate the effect of shAAT on NNK treatment, western blot, and densitometric analysis were performed. The expression levels of AAT and FGF-2 were statistically increased by NNK treatment in A549 cells (Con), while such increases in AAT expression were cancelled out in shAAT-transfected cells (shAAT) (Figure 5B). In addition, the effects of AAT on cancer cell migration and invasion were also determined. As shown, a significant decrease in cancer cell migration (Figure 5C) and invasion (Figure 5D) were observed in AAT down-regulating cells compared to control and scramble-transfected cells. For a better understanding, refer to Figure 5C, *right panel*, which summarizes the migration patterns of only 80,000 cells/well among diverse cell numbers. Interestingly, adhesion of the shAAT-transfected cells to the bottom of the upper chamber seemed to have decreased after 80 hours during invasion assay (*red arrow* in Figure 5D). Regarding this, western blot and immunofluorescence assays of representative adhesion molecules such as ICAM-1 and epithelial cellular adhesion molecule (EpCAM) were

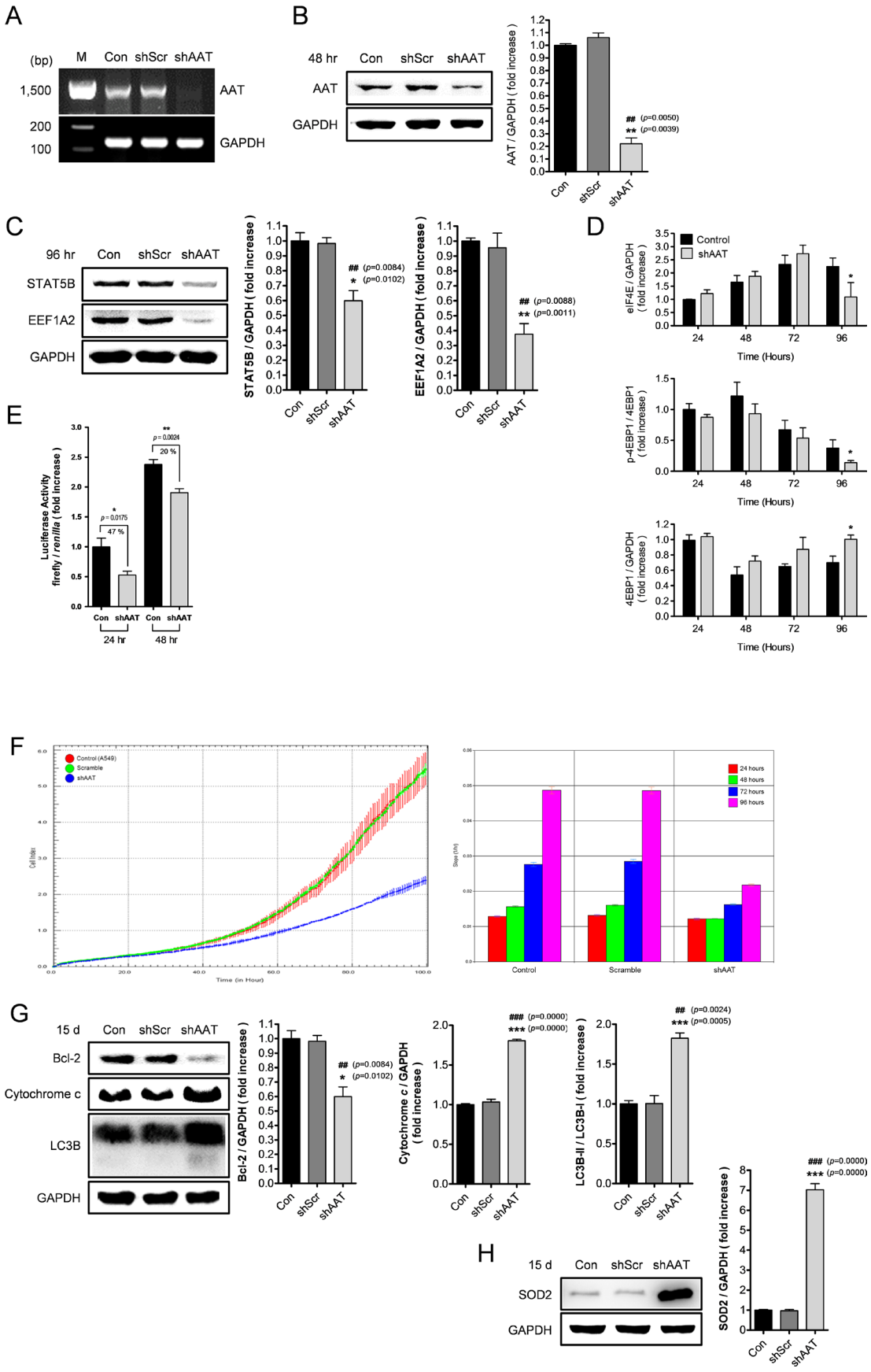
A
(bp)
M
Con
shScr
shAAT
1,500
200
100
AAT
GAPDH
B
48 hr
Con
shScr
shAAT
AAT
GAPDH
AAT / GAPDH (fold increase)
(p=0.0050)
** (p=0.0039)
C
96 hr
Con
shScr
shAAT
STAT5B
EEF1A2
GAPDH
STAT5B / GAPDH (fold increase)
(p=0.0084)
* (p=0.0102)
EEF1A2 / GAPDH (fold increase)
(p=0.0088)
** (p=0.0011)
D
Control
shAAT
eIF4E / GAPDH (fold increase)
Time (Hours)
p-4EBP1 / 4EBP1 (fold increase)
4EBP1 / GAPDH (fold increase)
E
Luciferase Activity firefly / renilla (fold increase)
p = 0.0175
47 %
p = 0.0024
20 %
Con
shAAT
24 hr
48 hr
F
Control (A549)
Scramble
shAAT
Cell Index
Time (in Hour)
24 hours
48 hours
72 hours
96 hours
Slope (/hr)
Control
Scramble
shAAT
G
15 d
Con
shScr
shAAT
Bcl-2
Cytochrome c
LC3B
GAPDH
Bcl-2 / GAPDH (fold increase)
(p=0.0084)
* (p=0.0102)
Cytochrome c / GAPDH (fold increase)
(p=0.0000)
*** (p=0.0000)
LC3B-II / LC3B-I (fold increase)
(p=0.0024)
*** (p=0.0005)
H
15 d
Con
shScr
shAAT
SOD2
GAPDH
SOD2 / GAPDH (fold increase)
(p=0.0000)
*** (p=0.0000)

(*Continued*)

Figure 4: Down-regulation of AAT suppresses cell survival through regulation of protein translation and cell death in lung carcinoma A549 cell. A. RT-PCR analysis of human AAT. Stably down-regulated cells were cultured for 24 hours and total RNA from cultured cells was isolated, then subjected to RT-PCR. M represents 100-bp molecular marker. Con = A549 cell; shScr = shScramble. **B.** Western blot analysis of human AAT. Cell lysates were subjected to western blot. Blots were probed with AAT antibody. *Right panel*) Densitometric analysis of the AAT western blot results. Values are the means ± SEM ($n = 3$). $^{**}p<0.01$ *vs.* Con and $^{\#\#}p<0.01$ *vs.* shScr. **C.** Western blot analyses of STAT5B and EEF1A2. Cell lysates were subjected to western blot analysis. Blots were probed with antibody of STAT5B or EEF1A2. **D.** Effect of shAAT on protein translation. Cell lysates were subjected to western blot analysis. Blots were probed with antibodies as indicated and densitometric analyses of the western blot results were performed. Values are the means ± SEM ($n = 3$). $^{*}p<0.05$ *vs.* Control of 96 hours. **E.** Effect of shAAT on cap-dependent translation. Cells were transfected with bicistronic reporter construct and incubated for 24 or 48 hours. Values are the means ± SEM ($n = 5$). $^{*}p<0.05$ or $^{**}p<0.01$ *vs.* Con. **F.** Real-time cell proliferation assay in A549 cells with down-regulated AAT, scramble, or control. Stably expressed cells were measured using an xCELLigence RTCA DP system for 96 hours. *Right panel*) Cell proliferation result at 24, 48, 72, and 96 hours in A549 cells with down-regulated AAT, scramble, or control. **G.** Effect of shAAT on cell death-related proteins. Cell lysates were subjected to western blot analysis. Blots were probed with antibodies as indicated. *Right panel*) Densitometric analyses of the Bcl-2, cytochrome *c*, and LC3B western blot result. Values are the means ± SEM ($n = 3$). $^{*}p<0.05$ or $^{***}p<0.001$ *vs.* Con; $^{\#\#}p<0.01$ or $^{\#\#\#}p<0.001$ *vs.* shScr. **H.** Effect of shAAT on SOD2 protein expression. Cell lysates were subjected to western blot analysis. Blots were probed with antibody of SOD2. *Right panel*) Densitometric analysis of the SOD2 western blot result. Values are the means ± SEM ($n = 3$). $^{***}p<0.001$ *vs.* Con, $^{\#\#\#}p<0.001$ *vs.* shScr.

performed in order to evaluate potential effects of shAAT on cell adhesion. Decreased expression levels of ICAM-1 and EpCAM were observed in AAT down-regulating cells compared to control or scramble-transfected cells (Figure 5E and 5F). Furthermore, the effect of shAAT on cancer-related proteins was evaluated using human oncology array and densitometric analysis in A549 cells with stable AAT down-regulation. The expression levels of cancer-related proteins were decreased at 96 hours in AAT down-regulating A549 cells compared to control A549 cells [CD31/PECAM-1 (66.42%), THBS1 (50.64%), MMP-2 (37.53%), MMP-9 (49.37)] (Supplementary Figure S6A and S6B). Additionally, to determine whether AAT overexpression induces metastasis in lung cancer, AAT-overexpressing A549 cell was used for western blot, densitometric analysis, and migration array. The increase of expression level of AAT, ICAM-1, and FGF-2 (Figure 5G) and migration (Figure 5H) were observed in AAT-overexpressing cells compared to control and vector-transfected cells. These results demonstrated that the down-regulation of AAT suppressed angiogenesis, migration, and invasion of lung cancer cells. Moreover, down-regulation of AAT could induce cell death through disruption of cancer cell adhesion.

Down-regulation of AAT suppresses lung tumorigenesis through inhibition of angiogenesis and cancer cell proliferation in the lungs of K-*ras*^{LA1} mice

The *in vivo* effect of shAAT was examined using murine lung cancer model, K-*ras*^{LA1} mice. To determine the silencing efficiency of shRNA constructs against murine AAT, RT-PCR, western blot, and immunostaining of AAT were carried out in the lungs of K-*ras*^{LA1} mice. The aerosol delivery of shAAT significantly decreased AAT mRNA and protein levels compared to control (Con) and scramble-delivered (shScr) groups (Figure 6A and 6B). Immunofluorescence image (Figure 6B, *lower panel*) of AAT further confirmed the RT-PCR and western blot results. Whether down-regulation of AAT would alter angiogenesis and adhesion in the lungs of K-*ras*^{LA1} mice were also assessed. Western blot analysis was carried out in the lungs of K-*ras*^{LA1} mice. The protein levels of THBS1, ICAM-1, and FGF-2 were significantly decreased in the lungs of shAAT-delivered mice compared to the scramble (shScr) and control mice (Figure 6C). The effect of shAAT on cancer cell proliferation was also investigated. Decreased levels of PECAM-1/CD31 and PCNA (proliferating cell nuclear antigen; cancer cell proliferative marker) were observed by western blot and immunohistochemistry (IHC) analysis in the lungs of shAAT-delivered mice (Figure 6D). Finally, total tumor number and volume in the lungs of 14-week-old K-*ras*^{LA1} mice were significantly decreased by the aerosol delivery of shAAT (Figure 6E). The suppression of lung tumor formation was further confirmed by H&E staining (Figure 6E, *lower panel*). Taken together, our work demonstrated that down-regulation of AAT suppressed lung cancer through inhibition of cell proliferation and angiogenesis in the lungs of K-*ras*^{LA1} mice.

DISCUSSION

Regardless of recent efforts, there are limited reports of AAT-related research on lung cancer. Some findings have demonstrated a positive correlation between serum concentration of AAT and the risk of lung cancer [4], while others have associated genetic AAT deficiency with an increased risk of lung cancer development [25]. Despite this, few studies have investigated the role of AAT in lung cancer. Moreover, there has been little study on AAT relevance in terms of lung cancer therapies.

Alpha1 proteinase inhibitor (human), GLASSIA, has been used for chronic augmentation and maintenance

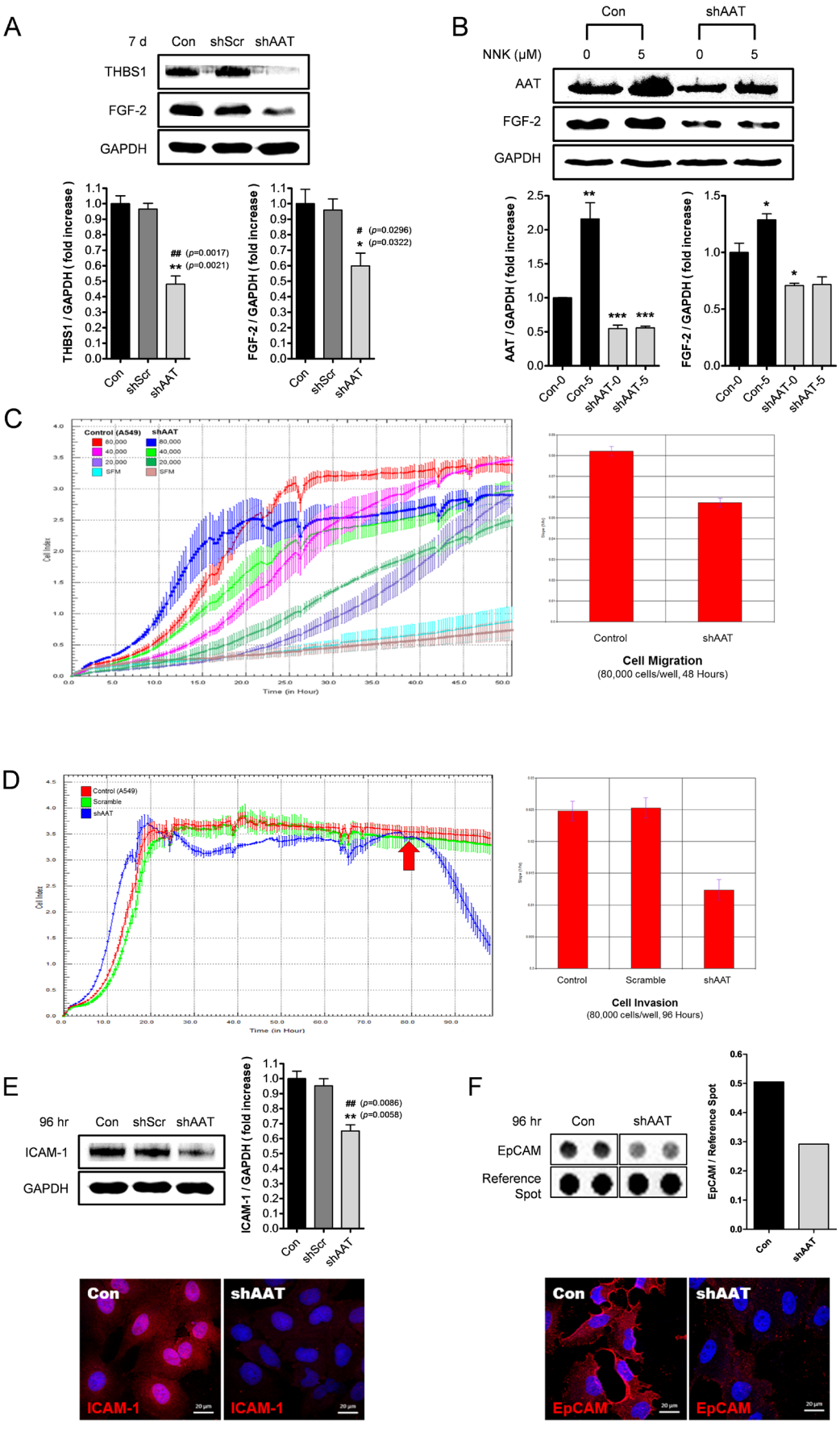
A
7 d
Con
shScr
shAAT
THBS1
FGF-2
GAPDH
THBS1 / GAPDH (fold increase)
(p=0.0017)
** (p=0.0021)
FGF-2 / GAPDH (fold increase)
(p=0.0296)
* (p=0.0322)
B
Con
shAAT
NNK (μM)
0
5
0
5
AAT
FGF-2
GAPDH
AAT / GAPDH (fold increase)
FGF-2 / GAPDH (fold increase)
Con-0
Con-5
shAAT-0
shAAT-5
C
Control (A549)
shAAT
80,000
40,000
20,000
SFM
Cell Index
Time (in Hour)
Control
shAAT
Cell Migration
(80,000 cells/well, 48 Hours)
D
Control (A549)
Scramble
shAAT
Cell Index
Time (in Hour)
Control
Scramble
shAAT
Cell Invasion
(80,000 cells/well, 96 Hours)
E
96 hr
Con
shScr
shAAT
ICAM-1
GAPDH
ICAM-1 / GAPDH (fold increase)
(p=0.0086)
** (p=0.0058)
Con
ICAM-1
shAAT
ICAM-1
F
96 hr
Con
shAAT
EpCAM
Reference Spot
EpCAM / Reference Spot
Con
shAAT
Con
EpCAM
shAAT
EpCAM

(*Continued*)

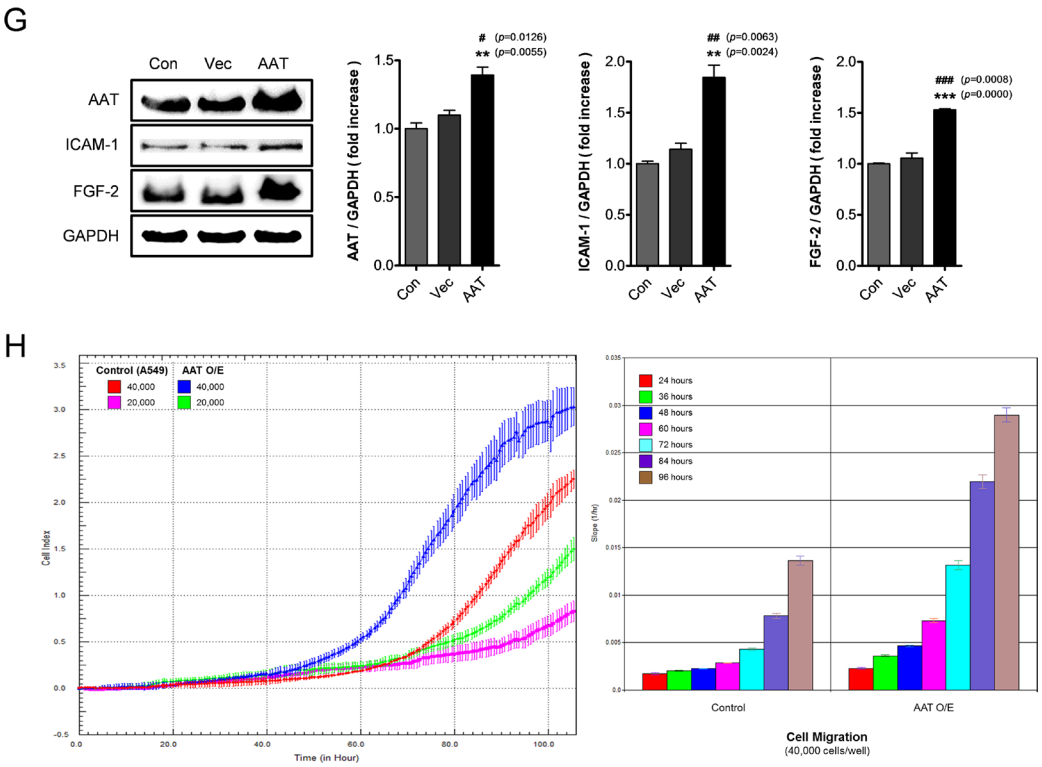

Figure 5: Down-regulation of AAT suppresses angiogenesis, migration, invasion, and adhesion in lung carcinoma A549 cell. A. Western blot analysis of angiogenesis-related proteins. Cell lysates were subjected to western blot analysis. Blots were probed with antibodies as indicated. *Lower panel*) Densitometric analyses of the THBS1 and FGF-2 western blot result. Values are the means ± SEM ($n = 3$). $^{*}p<0.05$ or $^{**}p<0.01$ *vs.* Con (control); $^{\#}p<0.05$ or $^{\#\#}p<0.01$ *vs.* shScr (shScramble). **B.** Effect of shAAT on NNK-induced AAT and FGF-2 expression. Cells were treated with NNK for 7 days and cell lysates were subjected to western blot analysis. Blots were probed with indicated antibodies. *Lower panel*) Densitometric analyses of the AAT and FGF-2 western blot result. Values are the means ± SEM ($n = 3$). $^{*}p<0.05$, $^{**}p<0.01$ or $^{**}p<0.01$ *vs.* Con (0). **C.** Real-time cell migration assay in A549 cells with down-regulated AAT or control. Stably expressed cells were measured using an xCELLigence RTCA DP system for 48 hours and densitometric analysis was performed for 80,000 cells. **D.** Real-time cell invasion assay in A549 cells with down-regulated AAT, scramble, or control. Stably expressed cells were measured using an xCELLigence RTCA DP system for 96 hours and densitometric analysis was performed. **E, F.** Effect of shAAT on cellular adhesion molecules. Cell lysates were subjected to (E) western blot analysis (for ICAM-1) or (F) Human XL Oncology Array (for EpCAM). Blots were probed with indicated antibody. *Right panels*) Densitometric analysis of the ICAM-1 western blot or EpCAM array result. (E) Values are the means ± SEM ($n = 3$). $^{**}p<0.01$ or $^{\#\#}p<0.01$ *vs.* Con. For immunofluorescence analysis, stably expressed cells were incubated for 96 hours, followed by fixing and immunostaining for ICAM-1 or EpCAM (red *via* Alexa Fluor 555) and nuclei (blue *via* DAPI). Con = A549 cell. The scale bars represent 10 μm. **G.** Effect of AAT on human lung adenocarcinoma cell line A549. Cell lysates were subjected to western blot analysis. Blots were probed with antibodies as indicated. *Right panel*) Densitometric analyses of the AAT, ICAM-1, and FGF-2 western blot result. Values are the means ± SEM ($n = 3$). $^{**}p<0.01$ or $^{***}p<0.001$ *vs.* Con; $^{\#}p<0.05$, $^{\#\#}p<0.01$ or $^{\#\#\#}p<0.001$ *vs.* Vec. **H.** Real-time cell migration assay in AAT-overexpressing A549 cells. Stably expressed cells were measured using an xCELLigence RTCA DP system for 110 hours. *Right panel*) Cell migration result at 24, 48, 72, and 96 hours in A549 cells with up-regulated AAT or control.

in adults that have emphysema due to severe congenital deficiency of AAT. GLASSIA increases antigenic and functional (anti-neutrophil elastase capacity, ANEC) serum levels and antigenic lung epithelial lining fluid levels of AAT. According to our results, the increase of AAT in patients with lung cancer might be responsible for facilitating lung tumor. Therefore, the use of appropriate dose of AAT as a therapeutic drug could be an essential subject of further research.

Chang et al. [5] reported AAT-mediated migration and invasion abilities (but not proliferation) in two kinds of lung adenoma cell lines (CL1-0 and CL1-5), which exhibited low and high metastatic properties, respectively. Our results, however, found that AAT overexpression facilitated the proliferation of normal lung cells (Figure 2E). Furthermore, we showed that shAAT inhibited cell proliferation in lung adenoma A549 cells (Figure 4F). Based on these results, we can suggest that AAT facilitates proliferation in normal lung cells, but not in lung adenoma cells. Moreover, our results strongly suggest that the removal of AAT in cancer cell/tissue may suppress the undesirable cell proliferation.

AAT is also known as a post-Golgi secretory pathway marker in INS-1 pancreatic β cells, which stably express wild-type AAT [26]. On the basis of the proteomics results (Table 1), induction of GOPC by AAT overexpression was confirmed. This was further supported by additional study of AAT C-terminal 44 deletion mutant form on AAT and GOPC (Supplementary Figure S3B). As described earlier, the PDZ domain of GOPC binds with BECN1 to induce autophagy. In order to determine the direct binding of GOPC and BECN1 in the present study, we examined the IP and *in situ* PLA in L132 cells, and confirmed binding affinity of these two proteins (Supplementary Figure S3C and S3D). In the PLA results, the number of dots to binding did not show significant differences due to the increase of GOPC in conjunction with the decrease of BECN1 by

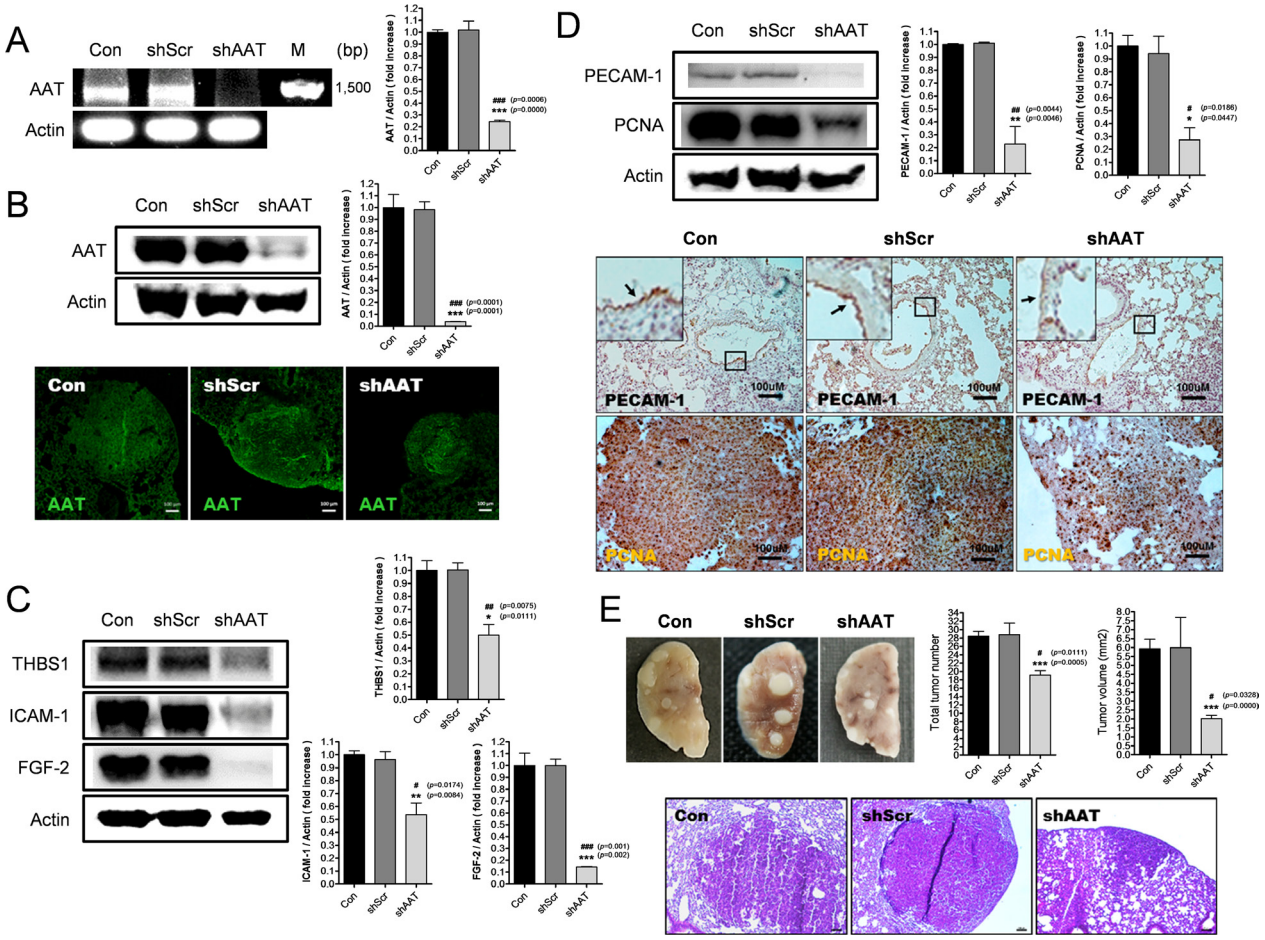

Figure 6: Down-regulation of AAT suppresses angiogenesis, cancer proliferation, and tumor formation in the lungs of K-*ras*^{LA1} mice. A. RT-PCR analysis of mouse AAT. Total RNA from lung tissue was isolated, then subjected to RT-PCR. M represents 100-bp molecular marker. *Right panel*) Densitometric analysis of the AAT RT-PCR result. Values are the means ± SEM (n = 3). $^{***}p$<0.001 *vs.* Con (control) and $^{\#\#}p$<0.01 *vs.* shScr (shScramble). **B.** Western blot analysis of mouse AAT. Lung tissue homogenates were subjected to western blot analysis. Blots were probed with antibody of AAT. *Right panel*) Densitometric analysis of the AAT western blot result. Values are the means ± SEM (n = 3). $^{***}p$<0.001 *vs.* Con, $^{\#\#\#}p$<0.001 *vs.* shScr. *Lower panel*) Immunofluorescence of AAT in the lungs. Green color (*via* Alexa Fluor 488) indicates AAT expression. The scale bars represent 100 μm. **C.** Western blot analyses of angiogenesis-related proteins. Lung tissue homogenates were subjected to western blot analysis. Blots were probed with antibodies as indicated. *Right panel*) Densitometric analyses of the THBS1, ICAM-1, and FGF-2 western blot result. Values are the means ± SEM (n = 3). $^{*}p$<0.05 or $^{***}p$<0.001 *vs.* Con; $^{\#}p$<0.05 or $^{\#\#\#}p$<0.001 *vs.* shScr. **D.** Western blot analyses of PECAM-1 and PCNA. Lung tissue homogenates were subjected to western blot analysis. Blots were probed with antibodies as indicated. *Right panel*) Densitometric analyses of the PECAM-1 and PCNA western blot result. Values are the means ± SEM (n = 3). $^{*}p$<0.05 or $^{**}p$<0.01 *vs.* Con; $^{\#}p$<0.05 or $^{\#\#}p$<0.01 *vs.* shScr. *Lower panel*) Immunohistochemistry of PECAM-1 and PCNA in the lungs. Dark brown color indicates PECAM-1 or PCNA expression. The scale bars represent 100 μm. **E.** Tumor formation in the lungs. Diverse size of white lumps indicates the tumor mass in the lungs of K-*ras*^{LA1} mice. *Right panel*) Total tumor number and tumor volume in the lungs. The mean tumor diameter of at least 1.0 mm was counted in the lungs of 14-week-old K-*ras*^{LA1} mice. Values are the means ± SEM (n = 5). $^{***}p$<0.001 *vs.* Con, $^{\#}p$<0.05 *vs.* shScr. *Lower panel*) Histological examination of lungs. The scale bars represent 100 μm.

AAT overexpression. This suggests that the increase of GOPC by AAT overexpression may be responsible for the inhibition of BECN1. Previously, our group reported that BECN1 induced autophagy and apoptosis in lung cancer model mice [27]. Moreover, several lines of evidence have indicated that there might be precise cross-talk or mutual function between autophagy and apoptosis [28, 29]. In the current study, autophagy and apoptosis were both decreased by AAT up-regulation (Figure 2H-2L). Furthermore, AAT-overexpressing cells survived longer compared to control cells when placed under starvation conditions (Supplementary Figure S4). Taken together, AAT may stimulate the cell survival by controlling autophagy or apoptosis through correlating with vesicle-mediated protein GOPC.

Another interesting result was the AAT-dependent change (Figure 2M and 4H) of SOD2, which catalyzes the dismutation of superoxide radicals into hydrogen peroxide and protects against oxidative stress in lung cells [30]. Indeed, overexpression of SOD2 has been associated with a marked suppression of cell growth in pancreatic adenocarcinoma [31] and breast cancer cells [32]. Very recently, SOD2 as a biomarker of different human diseases has been proposed as a new therapeutic application for cancer prevention and treatment [33]. Again, our study demonstrated that SOD2 was decreased by AAT overexpression (Figure 2I) while AAT down-regulation significantly increased the protein level of AAT (Figure 4H), which strongly indicates the AAT-dependent tumor suppressor function of SOD2. However, further studies are needed to define the precise link between AAT and SOD2.

THBS1 and TGF-β1 are known to promote plasminogen activator inhibitor type 1 (PAI-1, Serpin E1) production and to stimulate tumor cell attachment in human A549 lung carcinoma cells [34]. In addition, THBS1 and TGF-β1 have been found to induce flattened and spread appearance in human MDA-MB-231 breast carcinoma cells [35]. Our results showed that the expression of THBS1 and TGF-β1 by up- or down-regulation of AAT affected cell attachment (Figure 3 and 5). CAMs play an important role in cancer progression and metastasis [36]. The immunoglobulin superfamily of adhesion molecules consists of over 70 members, and some well-known members of the immunoglobulin superfamily for cell adhesive interactions are ICAM and VCAM. ICAM and VCAM are the most interesting target molecules in tumor cell metastasis because they are involved in tumor cell-endothelial cell interactions. Indeed, recent lines of evidence have shown that cancer metastasis of hepatocellular carcinoma (HCC) [37] and breast cancer cells [38] are correlated to ICAM-1 expression. Moreover, VCAM-1 has been increasingly reported as a therapeutic target in tumorigenicity and metastasis [39]. In this regard, our oncology array result indicated that a down-regulation of AAT suppressed lung cancer growth by decreasing the cell attachment-related proteins [PECAM-1/CD31 (66.42%), VCAM-1/CD106 (50.04%), CEACAM-5/CD66e (39.99%), VE-Cadherin (21.53%), E-Cadherin (17.23%), EpCAM/TROP1 (15.51%), and ICAM-1/CD54 (12.05%)] (Supplementary Figure S6B).

The nose-only inhalation system, adopted for the present study, is one of the very efficient methods for lung cancer gene delivery or therapy. Our previous studies have shown that aerosol delivery of target genes exhibits excellent and constant effects on lung tumorigenesis [11, 40, 42]. The present *in vivo* results demonstrated that the down-regulation of AAT decreased THBS1 expression, which could lead to inhibition of angiogenesis and metastasis (Figure 6C). Moreover, we showed suppression of cancer cell proliferation and tumorigenesis in the lungs of shAAT-delivered K-*ras*^{LA1} mice (Figure 6D and 6E). Together, our study indicated that suppression of angiogenesis could inhibit tumor growth in the lungs of shAAT-delivered K-*ras*^{LA1} mice.

Taken together, our results indicate that the AAT activates cell survival through promoting cap-dependent translation, vesicle-mediated transport, and metastasis, therefore suggesting that the regulation of AAT may provide an alternative way to cope with lung cancer treatment as well as prevention.

MATERIALS AND METHODS

Materials

Recombinant human AAT was purchased from R&D Systems (Minneapolis, MN, USA). Nicotine-derived nitrosamine ketone (NNK) and THBS1 inhibitor LSKL were obtained from Toronto Research Chemicals (Toronto, Canada) and AnaSpec Inc. (Fremont, CA, USA), respectively. Chloroquine was purchased from Sigma-Aldrich (St. Louis, MO, USA).

Human and mouse samples

The biospecimens for this study were kindly provided by the Korea University Guro Hospital of Biobank, a member of the National Biobank of Korea. The experiments using human tissues were authorized by Seoul National University Institutional Review Board (SNUIRB-E1201/001-001). All mice used in this study were housed under animal protocols of Seoul National University guidelines and the study was approved by the Animal Care and Use Committee at Seoul National University (SNU-121017-1 and SNU-140707-3). Breeding A/J mice and K-*ras*^{LA1} mice, which are a model of human non-small cell lung cancer, were purchased from Joongang Laboratory Animal Inc. (Seoul, Korea) and Human Cancer Consortium-National Cancer Institute (Frederick, MD,

USA), respectively. The induction of lung tumors by NNK was performed as described prebiously [41]. To determine the effects of mouse shAAT (5′-GAC ATC CAC AAG TCC TTC CAA CAC CTC CT-3′) against lung cancer development, the 6-week-old male K-*ras*^{LA1} mice [11, 42] were divided into three groups (n = 5 per group). The control group was untreated. The other two groups were exposed to an aerosol containing lentivirus-scramble or -shAAT. After exposure for 8 weeks (twice a week), the mice were sacrificed and the lungs (pooled tumor) were collected for IHC and western blot analysis.

Cell culture and generation of AAT up- or down-regulated stable cell line

Human normal lung epithelial cell L132 was obtained from Korean Cell Line Bank (KCLB, Seoul, Korea) and human lung cancer cells from American Type Culture Collection ATCC, Rockville, MD, USA). NCI-H146, -H209, -H226, -H322, -H460, -H520, and -H522 cells were cultured in RPMI-1640 supplemented with 10% fetal bovine serum (FBS) and 1% penicillin/streptomycin (P/S) in a humidified incubator in an atmosphere of 5% CO_2 at 37°C. These cell lines were used at passage < 25 and periodically authenticated by checking of cell morphology, real-time proliferation, and mycoplasma contamination. L132 or A549 cell (1×10^6) was grown in a T25 flask and was transfected with each plasmid containing human AAT or shRNA (5′-CAG ATC CAT GAA GGC TTC CAG GAA CTC CT-3′; Catalog No. TG309541D) targeting human AAT (OriGene Technologies, Rockville, MD, USA) using TransIT^R-LT1 reagent (Mirus Bio, Madison, WI, USA). After transfection, each cell was selected with medium containing 400 μg/ml of G418 disulfate salt (Sigma-Aldrich, St. Louis, MO, USA) for human AAT overexpression or 1 μg/ml of puromycin (InvivoGen, San Diego, CA, USA) for shRNA transfection. L132 and selected stable cell lines (Vector/L132 and AAT/L132) or A549 and selected stable cell lines (shScramble/A549, shAAT/A549, Vector/A549 and AAT/A549) were grown in Dulbecco Modified Eagle Medium (DMEM; GibcoBRL, Grand Island, NY, USA) supplemented with 10% FBS and 1% P/S or Ham′s F-12 (GibcoBRL) with 10% FBS and 1% P/S (GibcoBRL), respectively.

Dual-luciferase reporter assay

For luciferase assay, cells were grown on 6-well plates and were transfected with bicistronic reporter plasmid (pcDNA-fLuc-polIRES-rLuc). After 24 or 48 hours incubation, cells were washed twice in ice-cold PBS and extracted in passive lysis buffer (Promega), and firefly and *renilla* luciferase activities were then measured using a Dual-Luciferase® Reporter Assay System (Promega).

Real-time cell proliferation, migration, and invasion assay

Real-time cell proliferation, migration, and invasion were measured using an xCELLigence RTCA DP system (Roche Applied Science, Indianapolis, IN, USA), which monitors cellular events in real-time without the incorporation of labels. Briefly, cells were placed into well of an E-plate 16 (for proliferation; 2.5×10^3 cells) or Matrigel-coating (Matrigel : serum free media, 1:40) of the upper chamber of CIM-plate 16 (for migration; $2\sim8\times10^4$ cells, for invasion; 8×10^4 cells) and incubated for indicated times.

Histology and immunohistochemistry (IHC)

After paraffin embedding, whole lung tissue was cut at a thickness of 3 μm and transferred to a Plus slide (Fisher Scientific, Pittsburgh, PA, USA). For histological analysis, slides were stained with hematoxylin and eosin (H&E). IHC was performed as described previously [42].

Separation of mitochondria and cytosol

Mitochondria and cytosol were separated by a Qproteome™ mitochondria isolation kit from QIAGEN (Germantown, MD, USA).

Caspase-3 activity assay

Caspase 3 Assay Kit (Abcam, Cambridge, MA, USA) was used for the analysis of caspase 3 activation according to the manufacturer's protocol.

Cell adhesion assay

Cell adhesion assay was performed using CytoSelect™ 48-Well Cell Adhesion Assay (ECM Array, CELL BIOLABS, INC.). Experimental procedure followed the manufacturer's protocol, and spectrophotometric absorbance at 560 nm was measured using an Epoch microplate spectrophotometer (BioTek Instruments, Inc., Winooski, VT, USA).

Human angiogenesis and oncology array

Proteome Profiler™ Human Angiogenesis Array Kit and Human XL Oncology Array Kit (R&D Systems, Minneapolis, MN, USA) were used for angiogenesis- or oncology-related protein detection according to the manufacturer's protocol. After detection, the bands-of-interest were measured using ATTO Software CS Analyzer 3.0 (ATTO Corp, Tokyo, Japan).

Statistical analysis

All statistical analyses were performed using GraphPad Software version 4.02 (San Diego, CA, USA). Data are given as mean ± SEM. Student's *t* test was used for comparison between two groups. A value of $*p < 0.05$ was considered significant and $**p < 0.01$ and $***p < 0.001$ highly significant. Quantification of western blot analysis was carried out using ATTO Software CS Analyzer 3.0 (ATTO Corp).

ACKNOWLEDGMENTS AND FUNDING

This work was supported by the National Research Foundation (NRF-2012M3A9B6055304) of the Ministry of Education, Science and Technology (MEST) in Korea. M.H. CHO was also partially supported by the Research Institute for Veterinary Science, Seoul National University. This study was supported through BK21 PLUS Program for Creative Veterinary Science Research. We wish to express thanks to the staff of the National Center for Inter-University Research Facilities (NCIRF) for their efforts and supports.

CONFLICTS OF INTEREST

No potential conflicts of interest were disclosed.

REFERENCES

1. Gettins PG. Serpin structure, mechanism, and function. Chem Rev 2002; 102:4751-4804.
2. Sandhaus RA, Turino G. Neutrophil elastase-mediated lung disease. COPD 2013; 10:60-63.
3. El-Akawi ZJ, Abu-Awad AM, Sharara AM, Khader Y. The importance of alpha-1 antitrypsin (alpha 1-AT) and neopterin serum levels in the evaluation of non-small cell lung and prostate cancer patients. Neuro Endocrinol Lett 2010; 31:113-116.
4. Zelvyte I, Wallmark A, Piitulainen E, Westin U, Janciauskiene S. Increased plasma levels of serine proteinase inhibitors in lung cancer patients. Anticancer Res 2004; 24:241-247.
5. Chang YH, Lee SH, Liao IC, Huang SH, Cheng HC, Liao PC. Secretomic analysis identifies alpha-1 antitrypsin (A1AT) as a required protein in cancer cell migration, invasion, and pericellular fibronectin assembly for facilitating lung colonization of lung adenocarcinoma cells. Mol Cell Proteomics 2012; 11:1320-1339.
6. Kataoka H, Uchino H, Iwamura T, Seiki M, Nabeshima K, Koono M. Enhanced tumor growth and invasiveness in vivo by a carboxyl-terminal fragment of alpha1-proteinase inhibitor generated by matrix metalloproteinases: a possible modulatory role in natural killer cytotoxicity. Am J Pathol 1999; 154:457-468.
7. Zelvyte I, Lindgren S, Janciauskiene S. Multiple effects of alpha1-antitrypsin on breast carcinoma MDA-MB 468 cell growth and invasiveness. Eur J Cancer Prev 2003; 12:117-124.
8. Mamane Y, Petroulakis E, LeBacquer O, Sonenberg N. mTOR, translation initiation and cancer. Oncogene 2006; 25:6416-622.
9. Yang SX, Hewitt SM, Steinberg SM, Liewehr DJ, Swain SM. Expression levels of eIF4E, VEGF, and cyclin D1, and correlation of eIF4E with VEGF and cyclin D1 in multi-tumor tissue microarray. Oncol Rep 2007; 17:281-287.
10. Fujimura K, Sasaki AT, Anderson P. Selenite targets eIF4E-binding protein-1 to inhibit translation initiation and induce the assembly of non-canonical stress granules. Nucleic Acids Res 2012; 40:8099-8110.
11. Chang SH, Kim JE, Lee JH, Minai-Tehrani A, Han K, Chae C, Cho YH, Yun JH, Park K, Kim YS, Cho MH. Aerosol delivery of eukaryotic translation initiation factor 4E-binding protein 1 effectively suppresses lung tumorigenesis in K-ras^{LA1} mice. Cancer Gene Ther 2013; 20:331-335.
12. Cheng J, Moyer BD, Milewski M, Loffing J, Ikeda M, Mickle JE, Cutting GR, Li M, Stanton BA, Guggino WB. A Golgi-associated PDZ domain protein modulates cystic fibrosis transmembrane regulator plasma membrane expression. J Biol Chem 2002; 277:3520-3529.
13. Joubert PE, Meiffren G, Grégoire IP, Pontini G, Richetta C, Flacher M, Azocar O, Vidalain PO, Vidal M, Lotteau V, Codogno P, Rabourdin-Combe C, Faure M. Autophagy induction by the pathogen receptor CD46. Cell Host Microbe 2009; 6:354-366.
14. Yue Z, Horton A, Bravin M, DeJager PL, Selimi F, Heintz N. A novel protein complex linking the delta 2 glutamate receptor and autophagy: implications for neurodegeneration in lurcher mice. Neuron 2002; 35:921-933.
15. Lawler J. Thrombospondin-1 as an endogenous inhibitor of angiogenesis and tumor growth. J Cell Mol Med 2002; 6:1-12.
16. Wang TN, Qian X, Granick MS, Solomon MP, Rothman VL, Berger DH, Tuszynski GP. Thrombospondin-1 (TSP-1) promotes the invasive properties of human breast cancer. J Surg Res 1996; 63:39-43.
17. Schultz-Cherry S, Lawler J, Murphy-Ullrich JE. The type 1 repeats of thrombospondin 1 activate latent transforming growth factor-beta. J Biol Chem 1994; 269:26783-26788.
18. Bein K, Simons M. Thrombospondin type 1 repeats interact with matrix metalloproteinase 2. Regulation of metalloproteinase activity. J Biol Chem 2000; 275:32167-32173.
19. Crawford SE, Stellmach V, Murphy-Ullrich JE, Ribeiro SM, Lawler J, Hynes RO, Boivin GP, Bouck N. Thrombospondin-1 is a major activator of TGF-beta1 in vivo. Cell 1998; 93:1159-1170.
20. Narizhneva NV, Razorenova OV, Podrez EA, Chen J, Chandrasekharan UM, DiCorleto PE, Plow EF, Topol EJ, Byzova TV. Thrombospondin-1 up-regulates expression of

cell adhesion molecules and promotes monocyte binding to endothelium. FASEB J 2005; 19:1158-1160.

21. Huang da W, Sherman BT, Lempicki RA. Systematic and integrative analysis of large gene lists using DAVID bioinformatics resources. Nat Protoc 2009; 4:44-57.
22. Shimizu S, Narita M, Tsujimoto Y. Bcl-2 family proteins regulate the release of apoptogenic cytochrome c by the mitochondrial channel VDAC. Nature 1999; 399:483-487.
23. Pattingre S, Tassa A, Qu X, Garuti R, Liang XH, Mizushima N, Packer M, Schneider MD, Levine B. Bcl-2 antiapoptotic proteins inhibit Beclin 1-dependent autophagy. Cell 2005; 122:927-939.
24. Oberley LW. Mechanism of the tumor suppressive effect of MnSOD overexpression. Biomed Pharmacother 2005; 59:143-148.
25. Yang P, Sun Z, Krowka MJ, Aubry MC, Bamlet WR, Wampfler JA, Thibodeau SN, Katzmann JA, Allen MS, Midthun DE, Marks RS, de Andrade M. Alpha1-antitrypsin deficiency carriers, tobacco smoke, chronic obstructive pulmonary disease, and lung cancer risk. Arch Intern Med 2008; 168:1097-1103.
26. Feng L, Arvan P. The trafficking of alpha 1-antitrypsin, a post-Golgi secretory pathway marker, in INS-1 pancreatic beta cells. J Biol Chem 2003; 278:31486-31494.
27. Shin JY, Hong SH, Kang B, Minai-Tehrani A, Cho MH. Overexpression of beclin1 induced autophagy and apoptosis in lungs of K-rasLA1 mice. Lung Cancer 2013; 81:362-370.
28. Chang SH, Lee HJ, Kang B, Yu KN, Minai-Tehrani A, Lee S, Kim SU, Cho MH. Methylmercury induces caspase-dependent apoptosis and autophagy in human neural stem cells. J Toxicol Sci 2013; 38:823-831.
29. Chang SH, Minai-Tehrani A, Shin JY, Park S, Kim JE, Yu KN, Hong SH, Hong CM, Lee KH, Beck GR Jr, Cho MH. Beclin1-induced autophagy abrogates radioresistance of lung cancer cells by suppressing osteopontin. J Radiat Res 2012; 53:422-432.
30. Robinson BH. The role of manganese superoxide dismutase in health and disease. J Inherit Metab Dis 1998; 21:598-603.
31. Cullen JJ, Weydert C, Hinkhouse MM, Ritchie J, Domann FE, Spitz D, Oberley LW. The role of manganese superoxide dismutase in the growth of pancreatic adenocarcinoma. Cancer Res 2003; 63:1297-1303.
32. Weydert CJ, Waugh TA, Ritchie JM, Iyer KS, Smith JL, Li L, Spitz DR, Oberley LW. Overexpression of manganese or copper-zinc superoxide dismutase inhibits breast cancer growth. Free Radic Biol Med 2006; 41:226-237.
33. Borrelli A, Schiattarella A, Bonelli P, Tuccillo FM, Buonaguro FM, Mancini A. The functional role of MnSOD as a biomarker of human diseases and therapeutic potential of a new isoform of a human recombinant MnSOD. Biomed Res Int 2014; 2014:1-11.
34. Albo D, Arnoletti JP, Castiglioni A, Granick MS, Solomon MP, Rothman VL, Tuszynski GP. Thrombospondin (TSP) and transforming growth factor beta 1 (TGF-beta) promote human A549 lung carcinoma cell plasminogen activator inhibitor type 1 (PAI-1) production and stimulate tumor cell attachment in vitro. Biochem Biophys Res Commun 1994; 203:857-865.
35. Arnoletti JP, Albo D, Granick MS, Solomon MP, Castiglioni A, Rothman VL, Tuszynski GP. Thrombospondin and transforming growth factor-beta 1 increase expression of urokinase-type plasminogen activator and plasminogen activator inhibitor-1 in human MDA-MB-231 breast cancer cells. Cancer 1995; 76:998-1005.
36. Bendas G, Borsig L. Cancer cell adhesion and metastasis: selectins, integrins, and the inhibitory potential of heparins. Int J Cell Biol 2012; 2012:1-10.
37. Zhu XW, Gong JP. Expression and role of icam-1 in the occurrence and development of hepatocellular carcinoma. Asian Pac J Cancer Prev 2013; 14:1579-1583.
38. Rosette C, Roth RB, Oeth P, Braun A, Kammerer S, Ekblom J, Denissenko MF. Role of ICAM1 in invasion of human breast cancer cells. Carcinogenesis 2005; 26:943-950.
39. Chen Q, Massagué J. Molecular pathways: VCAM-1 as a potential therapeutic target in metastasis. Clin Cancer Res 2012; 18:5520-5525.
40. Minai-Tehrani A, Chang SH, Kwon JT, Hwang SK, Kim JE, Shin JY, Yu KN, Park SJ, Jiang HL, Kim JH, Hong SH, Kang B, Kim D, Chae CH, Lee KH, Beck GR Jr, Cho MH. Aerosol delivery of lentivirus-mediated O-glycosylation mutant osteopontin suppresses lung tumorigenesis in K-ras (LA1) mice. Cell Oncol 2013; 36:15-26.
41. Lu G, Xiao H, Li GX, Picinich SC, Chen YK, Liu A, Lee MJ, Loy S, Yang CS. A gamma-tocopherol-rich mixture of tocopherols inhibits chemically induced lung tumorigenesis in A/J mice and xenograft tumor growth. Carcinogenesis 2010; 31:687-694.
42. Chang SH, Hong SH, Jiang HL, Minai-Tehrani A, Yu KN, Lee JH, KimJE, Shin JY, Kang B, Park S, Han K, Chae C, Cho MH. GOLGA2/GM130, cis-Golgi matrix protein, is a novel target of anticancer gene therapy. Mol Ther 2012; 20:2052-2063.